

Melt Castable Derivatives of Pentaerythritol Tetranitrate

Maximilian Benz,^[a] Thomas M. Klapötke,^{*[a]} Niklas Kölbl,^[a] Jürgen Kuch,^[a] Tobias Lenz,^[a] Ersel Parigi,^[a] and Jörg Stierstorfer^[a]

Abstract: In the search for high-performance and environmentally friendly energetic materials, the derivatization of known materials is an often-applied concept to fulfill modern-day demands. Surprisingly, the long known pentaerythritol tetranitrate (PETN) has only been derivatized to a limited extent. PETN shows a brought application in energetic materials or pharmaceuticals. In this work, the PETN backbone

is modified by introducing nitramine, ionic nitramine, amine, ionic amine and tetrazole functionalities. The obtained and structurally similar compounds allow good comparability and insights into functional group effects on sensitivity, thermal behavior and performance. The functionalizations result in melting points in the range of 64 to 126 °C. Some compounds are therefore potential candidates to replace toxic TNT.

Introduction

Since the discovery of nitroglycerin and PETN, organic nitrates have persisted in energetic materials to this day.^[1] The advantageous single-step synthesis from the associated alcohol leads to compounds with high density, good performance and acceptable thermal stability.^[2] Not only PETN but also the long-known compounds Lead azide, RDX/HMX and TNT have also remained in the industry to this day. Most of those materials used today show unfavorable properties (e.g., toxicity, high sensitivity, harmful to the environment) that one would like to eliminate.^[3] Replacements should fulfill the demand for thermal properties (melt castable or heat-resistant explosives), performance and sensitivity. Furthermore, technological advances and changes in the industry, such as the use of shock tubes, are changing the general demand for new materials.^[4]

With growing commitment, computational chemistry is attempting to enable more targeted synthesis. The prediction of melting points is also continuously improved. For example, it has been shown that the square of molar mass is directly proportional to the melting point of n-alkanes. Non-computational methods for more complex C,H,N,O halogen compounds are also available.^[5] However, due to the complex correlations only some properties can be calculated with meaningful uncertainty, e.g. the initiation by impact can occur by different mechanisms, different measurement standards are applied

worldwide and the deviations and influencing factors are large.^[6] This harms a deeper understanding of the topic. Fundamental understandings, like shock compression experiments on single crystals, that Prof. Gupta is seeking to obtain are associated with immense effort.^[7]

In this interdisciplinary field of understanding the connection between chemical composition and properties, this work contributes to the comparison of some prominent energetic groups: nitramine, ionic nitramine, amine, ionic amine, tetrazole and organic nitrate. Figure 1 shows a selection of research already done in this field. It is shown that the energetic liquid PETN derivatives **A** are less sensitive towards friction than PETN.^[8] The polynitramino PETN **B** synthesized by Shreeve et al. outperforms PETN due to its superior heat of formation and lower sensitivity.^[9] A more comparative study was performed on erythritol tetranitrate derivatives **C** by Lease and Manner et al. They were able to show that the mechanical sensitivity decreases in the order: azido-, nitrate-, nitramino erythritol.^[10] Melting points in a suitable range for melt-castable substances were also achieved. In advance of this study, our group has been working on azidopentaerythritol derivatives **D**.^[11]

This shows that the introduction of azides lowers the melting point and increases the mechanical sensitivity. The group of Chavez et al. synthesized **SMX** with an ideal melting point at 85 °C–86 °C and twice the detonation pressure of TNT.^[12] However, the compound is sensitive and thermally not stable enough to be suitable as a TNT replacement. More energetic nitrates can be found in the review by Sabatini and Johnson.^[13] This includes the most prominent TNT replacement bis(1,2,4-oxadiazole)bis(methylene) dinitrate.^[14] Modification of one nitratomethyl function of the PETN backbone gives great comparability of the functional groups introduced. Furthermore, modification of PETN, with a melting point of 143 °C, will lead to lower melting and melt-castable explosives. The replacement of toxic TNT and the comparison of energetic functional groups is the goal of this work. Therefore azido, amino, ionic derivatives of amino, nitramino, ionic derivatives of nitramino and 1H-tetrazoles were introduced into the pentaerythritol body (Figure 2). Formally, in PETN, the C-bonded nitrate oxygen can be

[a] M. Benz, Prof. Dr. T. M. Klapötke, N. Kölbl, J. Kuch, T. Lenz, E. Parigi, Dr. J. Stierstorfer
 Department of Chemistry
 Ludwig Maximilian University of Munich
 Butenandstr. 5–13, 81337 München (Germany)
 E-mail: tmk@cup.uni-muenchen.de
 Homepage: <http://www.hedm.cup.uni-muenchen.de>

Supporting information for this article is available on the WWW under <https://doi.org/10.1002/chem.202204013>

© 2023 The Authors. Chemistry - A European Journal published by Wiley-VCH GmbH. This is an open access article under the terms of the Creative Commons Attribution License, which permits use, distribution and reproduction in any medium, provided the original work is properly cited.

Known Compounds

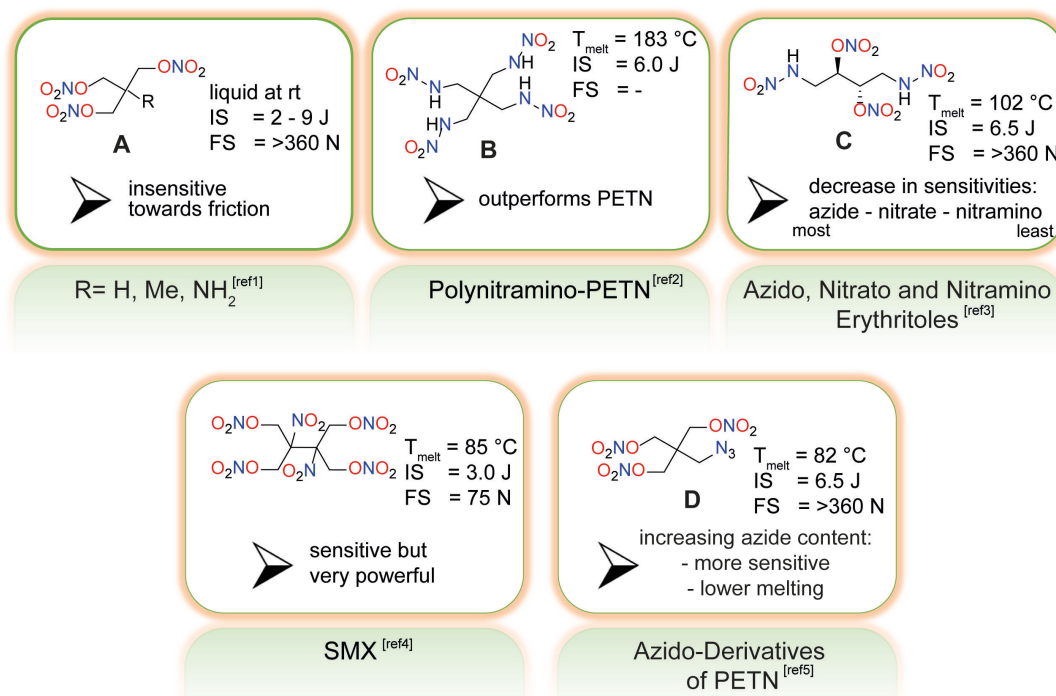


Figure 1. Selection of aliphatic energetic materials with various functionalities. (ref1: [8]; ref2: [9]; ref3: [10]; ref4: [12]; ref5: [11]).

Formal Modifications

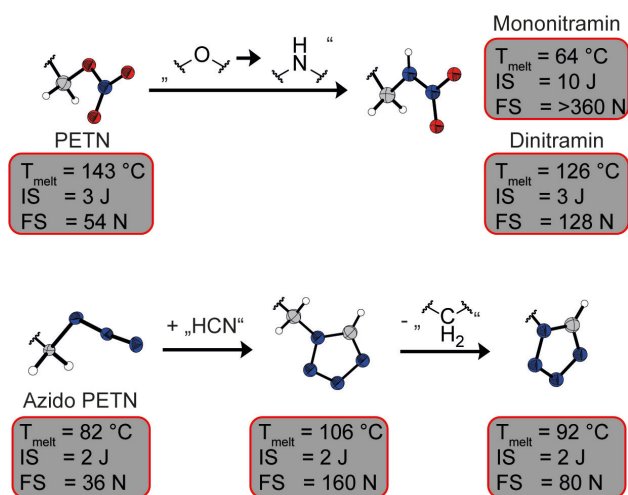


Figure 2. Selection of new compounds synthesized in this paper, together with their interrelationships and properties.

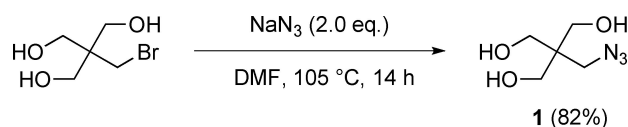
exchanged with an NH group to form the nitramine. Starting from the azido PETN, HCN can formally be added in a [2+3] cycloaddition to form a methyl-bridged tetrazole. The CH_2 group can now be formally removed to obtain a tetrazole bound to the central carbon.

Results and Discussion

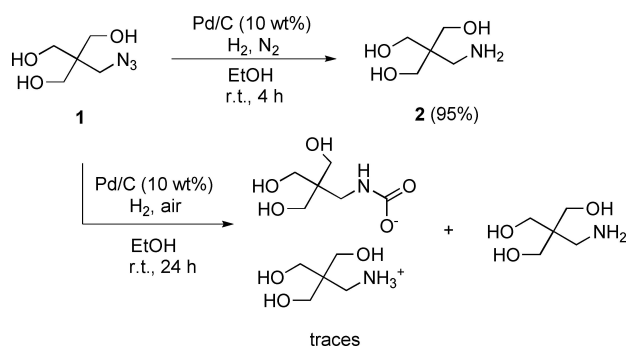
Synthesis

Safety: We have not experienced any incidents or accidental detonations of the compounds. But with the sensitivities present (between primary and secondary explosives), caution is advised. Working with small quantities and protection (kevlar gloves, ear protection, etc.) is strongly recommended.

New high energetic pentaerythritol tetranitrate derivatives were synthesized starting from the commercially available alcohol, pentaerythritol. Bromination yielded monobromopentaerythritol as reported.^[15] By a bromine-azide substitution, the reaction towards monoazidopentaerythritol **1** was performed similarly as previously reported by our group (Scheme 1).^[11] Compound **1** can be recrystallized from a mixture of ethyl acetate and chloroform. It is crucial to have a pure compound that is completely free of dimethylformamide for the following hydrogenation. Purification of the higher azides of pentaery-



Scheme 1. Synthesis of compound **1** starting from monobromopentaerythritol.

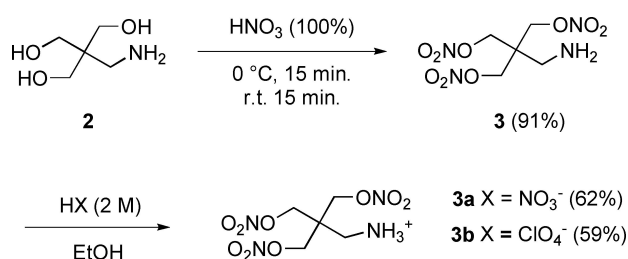


Scheme 2. Synthesis of compound 2 starting from 1.

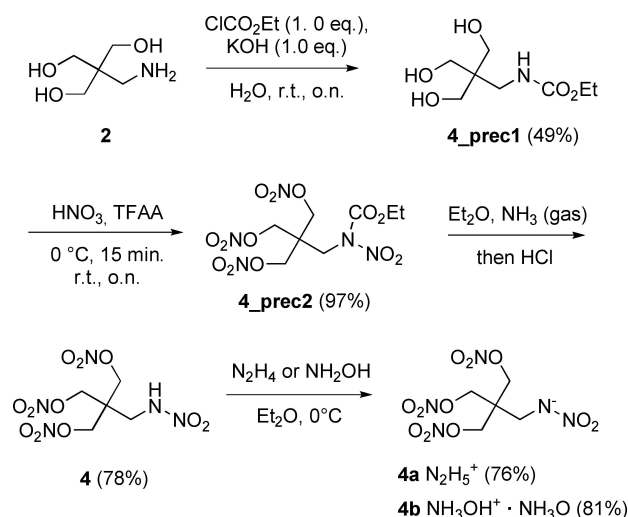
thritol is simpler as they are less water soluble and DMF can be separated much better by washing the organic phase with water.

Reduction of the azide using minimum amounts of palladium on charcoal (10%, 6 mg/mmol) (recovered and refreshed after the reaction) made the monoamine of pentaerythritol 2 accessible in quantitative yields as an off-white solid (Scheme 2). Other than previously reported, purification via the carbamate was not necessary when working under a nitrogen and hydrogen atmosphere.^[16] Nevertheless, the carbamate was discovered as a by-product of early experiments without using an inert gas (X-Ray Structure in the ESI). We achieved the best results by hydrogenation in ethanol with a constant flow of hydrogen over a few hours. The consumption of starting material was checked hourly by TLC.

Monoaminopentaerythritol trinitrate 3 was obtained in excellent yields as a yellowish viscous oil after nitration of 2 (Scheme 3). Purification by column chromatography did not remove the color or changes the physical state. Purification through the salt formation with hydrochloric acid in isopropanol yield the colorless chlorine salt that, when neutralized, gives colorless 2. Further derivatization through a different route was previously done by Hiskey and coworkers, giving the nitrate salt of monoaminopentaerythritol trinitrate 3a.^[16] We obtained compound 3a as a colorless solid through the reaction of 3 with diluted nitric acid. Furthermore, the colorless perchlorate salt 3b was obtained through the reaction of 3 with diluted perchloric acid (Scheme 3). In air, both compounds decompose within days, giving NO_x fumes.



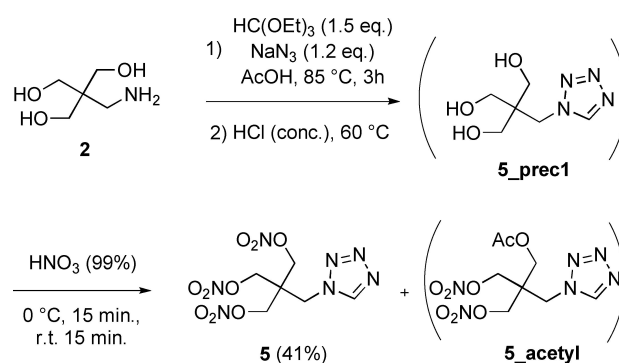
Scheme 3. Synthesis of compound 3 and its ionic derivatives 3a and 3b starting from 2.



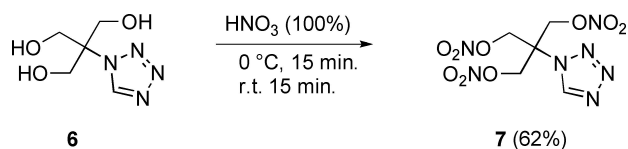
Scheme 4. Synthesis of compound 4 and its ionic derivatives 4a and 4b starting from 2.

The reaction of compound 3 to mononitraminopentaerythritol trinitrate 4 was challenging (Scheme 4). Direct nitration with nitric acid, acetyl nitrate or mixed acid did not yield the required nitramine in one step. The route previously applied by our group, Shreeve or Manner and coworkers was performed successfully to yield 4 in 37% overall yield.^[9,10b,17] First the amine is protected through a reaction with ethyl chloroformate. The protected amine 4_prec1 was then nitrated using a mixture of trifluoroacetic anhydride and nitric acid and the protected nitramine 4_prec2 was obtained as trinitrate. Deprotection with ammonia and precipitation through acidification in water yielded nitramine 4 as a colorless solid. The formation of ionic derivatives of 4 with equimolar amounts of ammonia and potassium hydroxide^[18] did not yield the desired salts in their pure form. The hydrazinium salt 4a and the hydroxylammonium salt with one cocrystalline ammonia oxide 4b could only be obtained by crystallization from ether at 4 °C (Scheme 4). Higher temperatures or protic solvents lead to impure products and decomposition.

Tetrazole ring closure at the amine of 2 was applied with Gaponik conditions (Scheme 5).^[19] The obtained crude 5_prec1



Scheme 5. Synthesis of compound 5 starting from 2.



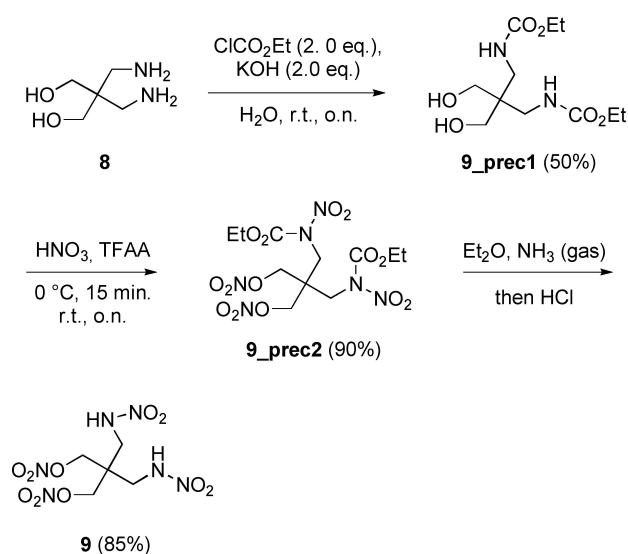
Scheme 6. Synthesis of compound 7 starting from 6.

was directly nitrated in fuming nitric acid. The less polar product was separated by column chromatography. A mono-acetylated side product **5_acetyl** could be identified by NMR and X-ray crystallography in reasonable amounts (ESI). To increase the yield of **5**, the crude intermediate **5_prec1** was heated in concentrated hydrochloric acid to remove the acetyl group before nitration. Thus, the yield was increased to an overall 41% starting from **2**.

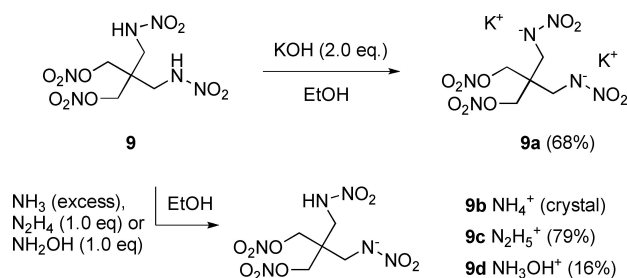
In advance, literature known compound **6** TRIS-alcohol was nitrated to its colorless TRIS-trinitrate **7** in moderate yields (Scheme 6). Isolation of **6** as pure solid showed to be complicated. Nevertheless, the purity of the starting material was not important for nitration to pure **7**.

Several complexation attempts of compounds **5** and **7** failed. No complexation with copper and manganese, nitrates or perchlorates was observed. Instead, the ligands crystallized again.

Attempts to synthesize di- or tri-substituted derivatives were made. During our work on the dinitramine **9**, similar results were published.^[10a] The synthesis is comparable to **4** (Scheme 4). The diamine **8** was further reacted to compound **9_prec1**. After nitration, the protected dinitramine **9_prec2** is yielded. Treatment with gaseous ammonia followed by acidification of the aqueous phase led to the precipitation of dinitraminopentaerythritol dinitrate **9** in very good yields (Scheme 7). Other than for compound **4**, crystal structure measurement with refinement of **9** was possible. Furthermore,



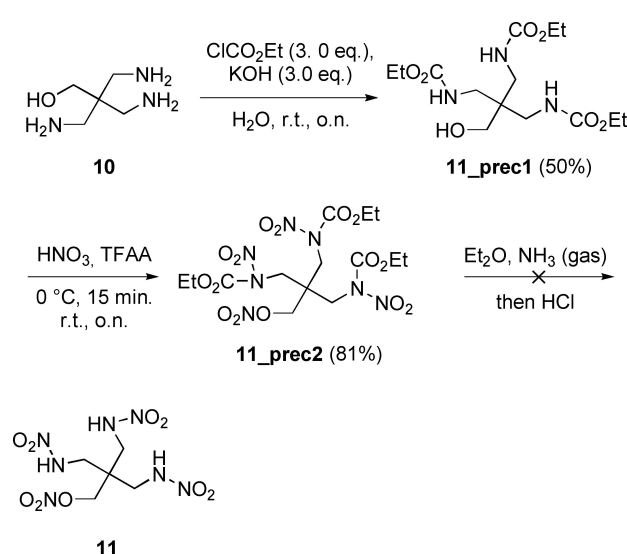
Scheme 7. Synthesis of compound 9 starting from 8.

Scheme 8. Ionic derivatives **9a–d** starting from **9**.

the reaction pathway is proven by crystal structures of the starting material **8** and the two intermediates **9_prec1** and **9_prec2**. Tetrazole ring closure of **8** with a similar procedure to compound **5**, resulted in the recovery of the starting material. Those reactions on diamino alkyl chains are known to show low yields for uneven chain length.

Ionic derivatives of acidic **9** were obtained by reaction with bases (Scheme 8). The potassium salt **9a** precipitates from an ethanolic solution of **9**. With the nitrogen bases ammonia, hydrazine and hydroxylamine only the mono salts could be obtained as they crystalize from ethanol. The ammonia salt **9b** could not be isolated, only a crystal structure was obtained (ESI). The hydrazine **9c** and hydroxylamine **9d** salts were fully characterized.

Furthermore, the tri derivatives were investigated (Scheme 9). Amine **10** was protected with ethyl chloroformate to yield **11_prec1**. The following nitration with trifluoroacetic anhydride yielded **11_prec2** as expected. Several deprotection attempts towards trinitramine **11** failed. Only an impure yellow oil that cannot be purified or reacted selectively is obtained.

Scheme 9. Attempt for the synthesis of **11**.

NMR spectroscopy

Investigation through ^1H and ^{13}C was performed on all compounds (ESI). It can be observed that O-nitration leads to a characteristic change in chemical shift. The shift of the protons of the CH_2 group nearby generally increases from ~ 3.3 to ~ 4.6 ppm and for tetrazole containing compounds from 3.9 to 5.3 ppm. The carbon shifts generally from 62 ppm to 71 ppm. In advance ^{15}N NMR of the compounds **4**, **5** and **7** were measured, revealing the chemical shifts of all nitrogen atoms contained (Figure 3). The nitrogen of all the organic nitrates is at -50 ppm. The nitramino nitrogens of **4** show at -20 ppm for the nitro group and -220 ppm for the amine bearing a proton. The tetrazole nitrogens of **5** and **7** are found between 20 and -170 ppm. The nitrogen bound to two carbons is shifted between -150 and -170 ppm, which matches with the shifts

of similar 1-alkyl-substituted tetrazoles.^[20] The nitrogen bound to only one carbon atom can be observed at -50 to -60 ppm. The more shielded nitrogen atoms are at about -25 ppm for N3 and 10 ppm for N4.

Crystal structures

The mono-substituted PETN derivatives **3a**, **3b**, **4a**, **4b**, **5** and **7** as well as the side products **2_CO₂** and **5_acetyl** were analyzed by low-temperature single crystal diffraction. For the disubstituted compounds structures of **8**, **9_prec1**, **9_prec2**, **9a** and **9b** were observed. The structures of **3a**, **4b**, **5**, **7** and **9** are discussed below (Figures 4–9). The structures of **2_CO₂**, **3b**, **4a**, **5_acetyl**, **9_prec1**, **9_prec2**, **9a** and **9b** together with all measurement parameters and refinement data can be found in

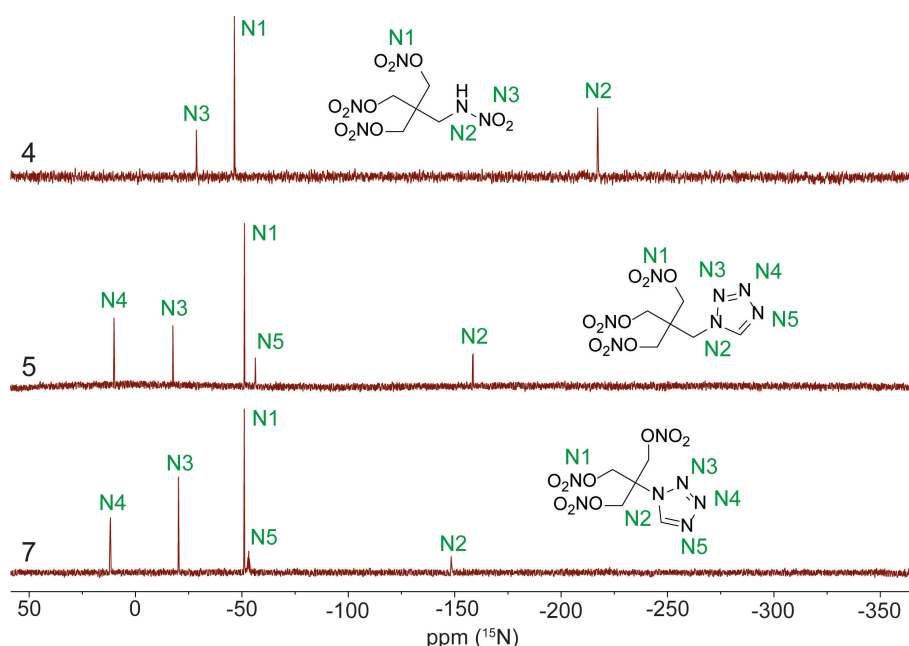


Figure 3. ^{15}N NMR spectra of **4**, **5** and **7** (Acetone- d_6 , 1H coupled).

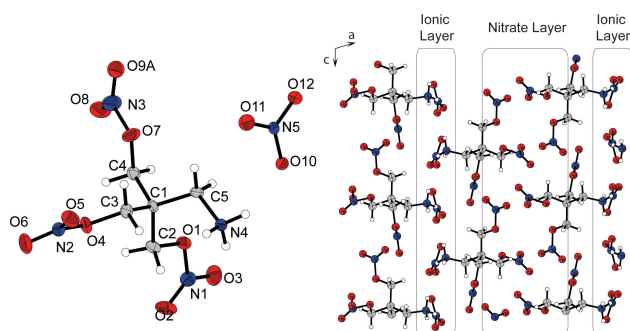


Figure 4. Scheme caption. Formula unit of **3a**. Selected bond length (Å): C1–C4: 1.537(8), C4–O7: 1.449(8), O7–N3: 1.384(8), N3–O8: 1.195(9), C1–C5: 1.530(8), C5–N4: 1.478(8), N5–O10: 1.252(7). Selected bond angles ($^\circ$): C5–C1–C4: 109.8(5), C1–C4–O7: 106.6(5), O7–N3–O8: 118.2(7), C1–C5–N4: 113.9(5), O10–N5–O11: 122.2(5).

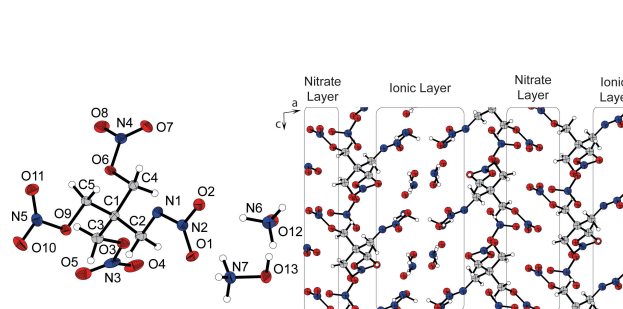


Figure 5. Formula unit of **4b**. Selected bond length (Å): C1–C4: 1.534(3), C4–O6: 1.451(3), O6–N4: 1.396(2), N4–O7: 1.200(3), C1–C2: 1.535(3), C2–N1: 1.458(3), N1–N2: 1.264(3), N2–O2: 1.312(2), N6–O12: 1.417(3), N7–O13: 1.421(3). Selected bond angles ($^\circ$): C2–C1–C4: 106.9(2), C1–C4–O6: 106.5(2), C4–O6–N4: 113.2(2), O6–N4–O7: 118.5(2), C1–C2–N1: 107.9(2), C2–N1–N2: 114.1(2), N1–N2–O1: 125.6(2).

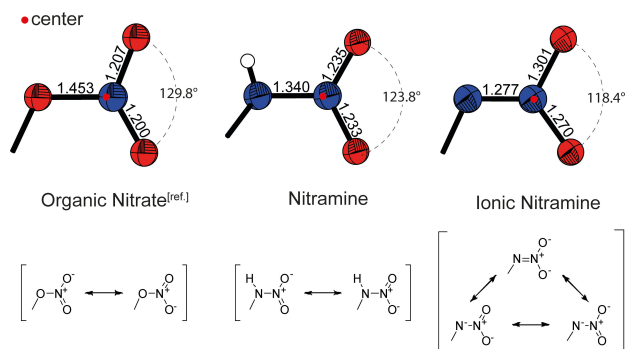


Figure 6. Comparison of bonding and angles of an organic nitrate of PETN, nitramine (**9**) and ionic nitramine (**4b**) with the resulting Lewis structures below.

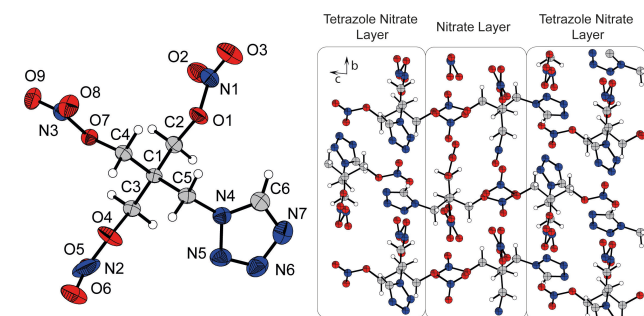


Figure 7. Formula unit of **5**. Selected bond length (Å): C1–C2: 1.5324(1), C2–O1: 1.4374(1), O1–N1: 1.4018(1), N1–O2: 1.2111(1), C1–C5: 1.5446(1), C5–N4: 1.4358(1). Selected bond angles [°]: C5–C1–C2: 112.35(1), C1–C2–O1: 106.06(1), C2–O1–N1: 114.99(1), O1–N1–O3: 111.61(1), C1–C5–N4: 114.84(1).

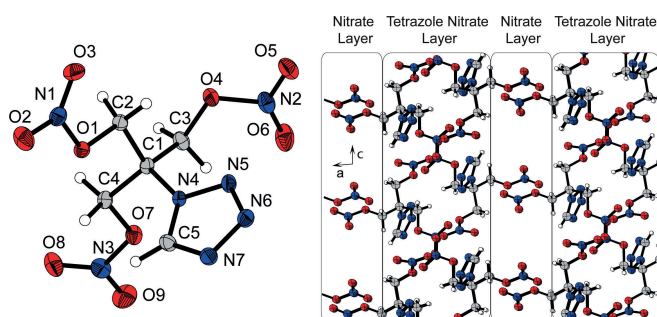


Figure 8. Formula unit of **7**. Selected bond length [Å]: C1–C3: 1.539(2), C3–O4: 1.440(1), O4–N2: 1.413(2), N2–O6: 1.200(2), C1–N4: 1.480(2). Selected bond angles [°]: N4–C1–C3: 110.6(1), C1–C3–O4: 109.9(1), C3–O4–N2: 115.1(1), O4–N2–O6: 119.0(1), N5–N4–C1: 120.7(1).

the Supporting Information. Compound **4** crystallizes in colorless blocks that are suitable for single-crystal diffraction. Due to the structural similarity of the nitrate and nitramino group, the molecules are highly disordered and refinement was impossible. Nevertheless, the structure is proven by the follow-up reactions to the ionic derivatives **4a** and **4b**. The datasets were uploaded to the CSD database and can be accessed free of charge. CSD Deposition numbers: 2232116–2232128.

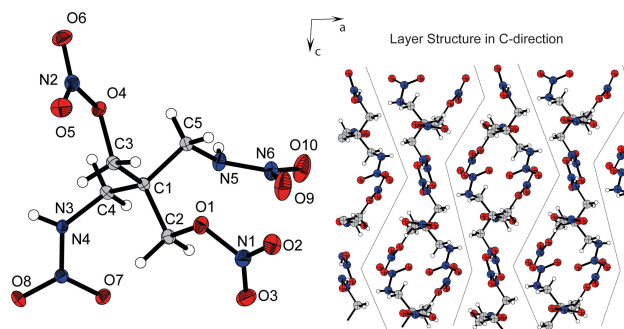


Figure 9. Formula unit of **9**. Selected bond length [Å]: C1–C3: 1.529(3), C3–O4: 1.455(2), O4–N2: 1.394(2), N2–O6: 1.206(2), C1–C5: 1.548(3), C5–N5: 1.455(3), N5–N6: 1.362(2), N6–O9: 1.237(3). Selected bond angles [°]: C1–C3–O4: 106.1(2), C1–C4–N3: 113.8(2), C3–O4–N2: 113.4(1), O5–N2–O6: 129.2(2), C5–N5–N6: 118.4(2), O9–N6–O1.

The nitrate salt **3a** crystallizes in the monoclinic space group $P2_1/c$ with eight molecules in the unit cell. A density of 1.660 g cm^{-3} at 293 K was determined. The four carbon atoms around the central carbon of the pentaerythritol backbone span a tetrahedron with a volume of 1.83 Å^3 . The C–C distances for the nitrate-bound carbons are 1.50–1.55 Å. The carbon-oxygen bonds are 1.45 Å long. The organic nitrate nitrogen is not in the center of the three oxygens. The N–O bond directed to the carbon-bound oxygen is about 0.20 Å longer than the remaining, 1.20 Å long. The bond between the ammonium functionality and carbon is 1.49 Å, longer than the nitrates are bound to carbon. The planar nitrate shows symmetrically distributed binding with an N–O bond length of 1.25 Å. The O–N–O angles are between 117° and 122° slightly off the ideal 120° because of attractive interactions with the ammonium proton. The three-dimensional structure viewed along the b -axis reveals ionic layers where the ammonium and nitrate are fixed by O–H interactions. Those layers alternate with layers fixed through nitrate-nitrate interactions (Figure 4).

The hydroxylammonium salt of mononitraminopentaerythritol trinitrate **4b** crystallizes with one molecule of ammonia oxide, in the triclinic space group $P-1$. The density is 1.687 g cm^{-3} at 100 K with four molecules in the unit cell. The tetrahedron in the center has a volume of 1.84 Å^3 . The bond length and angles of the carbon backbone and nitrate functionalities are comparable to compound **3a**. The C–N bond of the nitramine is shorter than that of the ammonium functionality in **3a** with a length of 1.46 Å close to the C–O bonds. In contrast to the nitrate group the nitrogen in the center of the planar nitramino group is well-centered with N–O or N–N bond lengths of 1.26–1.31 Å. The bond distances in the hydroxylammonium cation and the ammonia oxide are comparable with a length of 1.42 Å. In the three-dimensional structure again alternating layers can be observed when viewing along the b -axis. An ionic layer with the deprotonated nitramine and the cationic and neutral hydroxylamine is found. This layer is again alternating with layers of organic nitrates (Figure 5).

Since the electronic situation of several substituents is similar ($-\text{ONO}_2$, $-\text{NH}-\text{NO}_2$, $-\text{N}-\text{NO}_2$), we featured a comparison of those including the crystallographic key properties. In Figure 6 an organic nitrate of PETN, a nitramino group of **9** and an ionic nitramine of **4b** were analyzed and compared. The bond distance shortens from the nitrate (1.45 Å) to the nitramine (1.34 Å) to the anionic nitramine (1.28 Å). The central nitrogen initially shifted to the nitro group and moves further to the center (red dot). Consequently, the outer O–N–O angle changes and becomes smaller from 129.8° to 118.4°. The Lewis structures below clearly show that the N–N bond of the ionic nitramine has a double bond character and therefore must be shorter, which is proven here through the comparison of the bond lengths.

The N-tetrazole derivative of PETN **5** crystallizes in the triclinic space group $P\bar{1}$ with two molecules in the unit cell. The density at 123 K is 1.695 g cm^{-3} . The tetrahedron volume is 1.84–1.85 Å³. The angles and bond length of the nitrate bearing arms are comparable to the previous structures. The distance of N4 of the tetrazole to the pentaerythritol carbon is 1.44 Å and therefore shorter than the introduced functionality in **3a** and **4b**. The three-dimensional structure reveals a more rigid structure. Alternating layers can be observed along the *a*-axis. Nitrate-nitrate interactions are part of one layer and tetrazole N–H interactions are part of the other layer (Figure 7).

The trinitrate of the TRIS-tetrazole backbone **7** crystallizes in the monoclinic space group $P2_1/n$ with four molecules in the unit cell. With a density of 1.764 g cm^{-3} at 110 K, **7** shows the highest density of all investigated derivatives. The tetrahedron spanned by the tris-backbone has a volume of 1.80 Å³. Thus, the tetrahedron is smaller than that of all other derivatives. The angles and bond length of the nitratomethyl groups are comparable to the previously discussed. The bond distance of the central carbon to the tetrazole is 1.48 Å and therefore longer than the C–N bond in **5**. The three-dimensional structure, viewed along the *b*-axis, reveals a similar layer type to **5**. The nitrate layer is dominated by O–H interactions whereas

the tetrazole nitrate layer is dominated by N–H interactions (Figure 8).

Dinitraminopentaerythritol dinitrate **9** crystallizes in the monoclinic space group $P2_1/n$ with four molecules in the unit cell. The density of 1.790 g cm^{-3} at 123 K is higher than the density of the mono derivatives. The inner tetrahedron shows a volume of 1.87 Å³, the largest of all compounds. The carbon nitramin bond is 1.46 Å long and comparable to the C-nitrate or C-tetrazole distances. When a grown supercell is viewed along the *b*-axis, alternating zic-zac layers can be identified. The whole structure is dominated by CH–O and NH–O hydrogen bonding (Figure 9).

Physico chemical properties

The energetic properties and detonation parameters of compounds **3**, **3a**, **3b**, **4**, **4a**, **4b**, **5**, **7**, **9**, **9a**, **9c** and **9d** are presented in Table 1. All energetic products were analyzed by differential thermal analysis (DTA) with a heating rate of 5 K min^{-1} . The onset temperatures for endothermic and exothermic peaks were determined and are shown in Figure 10. For compounds **4**, **5** and **7** the melting and recrystallization of the melt were proven by optical observation. Pure PETN melts at 143 °C and decomposes shortly thereafter at 180 °C. For a melt cast energetic, it is important to achieve a melting range that can be reached with hot or boiling water possibly under pressure (80–120 °C). Furthermore, the decomposition point should be as far away as possible from the melting point to ensure safe processing. Since organic nitrates usually decompose around 180 °C (onset) and, on closer inspection, often earlier, the distance between melting and decomposition is the critical factor here.

Compounds **4**, **5** and **7** are therefore particularly suitable as melt-castable energetic materials. Compound **4** melts early at 64 °C and decomposes (106 °C higher) at 170 °C. Compound **5** has a significantly higher melting point of 106 °C and decomposition is 74 °C later at 180 °C. Nitratotetrazole **7** shows an

Table 1. Energetic properties and detonation parameters of MAPETN, **3**, **3a**, **3b**, **4**, **4a**, **4b**, **5**, **7**, **9** compared to PETN.

| | IS [J] ^[a] | FS [N] ^[b] | ρ [g cm^{-3}] ^[c] | Ω [%] ^[d] | $T_{\text{endo}}/T_{\text{exo}}$ [°C] ^[e] | $\Delta_f H^\circ$ [kJ mol^{-1}] ^[f] | P_{CJ} [kbar] ^[g] | V_{det} [m s^{-1}] ^[h] | TNT equiv. ^[i] |
|-----------|-----------------------|-----------------------|--|-----------------------------|--|--|---------------------------------------|---|---------------------------|
| TNT | > 15 | > 360 | 1.648 | −24.7 | 81/289 | −56 | 183 | 6785 | 1.01 |
| MAPETN | 2 | 36 | 1.667 | 0.0 | 82/180 | −59 | 278 | 8092 | 1.57 |
| 3 | 7.5 | > 360 | – | −5.9 | 89/153 | – | – | – | – |
| 3a | 3 | 120 | 1.659 | 7.2 | 145/145 | −423 | 287 | 8163 | 1.68 |
| 3b | – | – | 1.792 | 10.8 | –/146 | −383 | 317 | 8484 | 1.77 |
| 4 | 10 | > 360 | 1.729 ^{pyc} | 7.6 | 64/170 | −339 | 305 | 8283 | 1.56 |
| 4a | 3 | 120 | 1.637 | −2.3 | –/100 | −48 | 293 | 8363 | 1.88 |
| 4b | 4 | 45 | 1.709 | 2.1 | 73/73 | – | – | – | – |
| 5 | 2 | 160 | 1.652 | 0.0 | 106/180 | −48 | 252 | 7847 | 1.44 |
| 7 | 2 | 80 | 1.716 | 2.6 | 92/163 | −3 | 292 | 8258 | 1.52 |
| 9 | 3 | 128 | 1.744 | 0.0 | 126/134 | −254 | 302 | 8352 | 1.53 |
| 9a | 3 | > 360 | 1.856 | 4.1 | –/135 | – | – | – | – |
| 9c | 3 | 160 | – | 13.7 | –/108 | – | – | – | – |
| 9d | 15 | 360 | – | −3.2 | 120/125 | – | – | – | – |
| PETN | 3–4 | 54 | 1.778 | −10.1 | 143/180 | −484 | 313 | 8471 | 1.64 |

[a] Impact sensitivity (BAM drophammer (1 of 6)). [b] Friction sensitivity (BAM friction tester (1 of 6)). [c] From X-ray diffraction analysis recalculated to 298 K. [d] Oxygen balance with respect to CO. [e] Melting/Decomposition temperature (DTA; $\beta = 5^\circ\text{C min}^{-1}$). [f] Calculated enthalpy of formation (ExpLO5-V6.05.04 code). [g] Detonation pressure at Chapman-Jouguet point (ExpLO5-V6.05.04 code). [h] Detonation velocity. [i] TNT equiv. based on the Power Index.

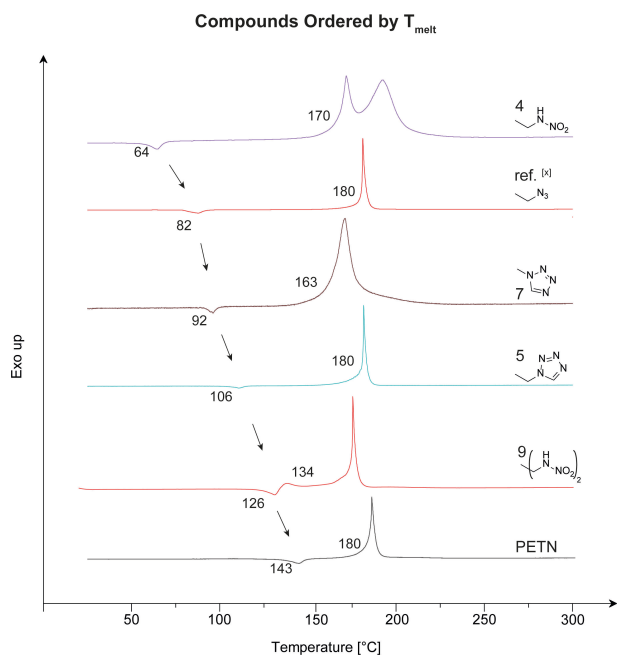


Figure 10. Differential thermal analysis of derivatives compared to PETN and monoazidopentaerythritol trinitrate.^[11]

ideal melting point at 92 °C and decomposition at 71 °C later. Interestingly compound **9** decomposes right after melting at 126 °C–134 °C. The formation of ionic derivatives as well as having a nucleophilic amino group lowers the thermal stability and leads to early decompositions below 150 °C.

The detonation parameters were calculated using the EXPLO5-V6.05.04 code. The densities were taken from the crystal structures and simply calculated to room temperature densities. The density of compound **7** is measured pycnometrically. The heat of formation is calculated from Gaussian CBS-4 M enthalpies using the atomization method (ESI). The melt cast candidates **4**, **5** and **7** outperform TNT by 1.0–1.5 km s⁻¹. The high densities of **4** and **7** cause them to be more powerful with a detonation velocity of 8.3 km s⁻¹, whereas **5** still shows a good detonation velocity of 7.8 km s⁻¹. The detonation pressures are at 25–31 GPa and correspond to the detonation velocities. The ionic derivatives show properties in the same area, with the perchlorate salt **3b** as the most powerful compound. With a velocity of 8.5 km s⁻¹ and a pressure of 31.7 GPa, it appears more powerful than PETN. TNT equivalents, based on the power index, were calculated from the heat of detonation and the volumes of gas at STP. All calculated compounds outperform TNT by 1.44 to 1.88 times. With the melt cast candidates being close to the power of PETN.

Conclusion

The PETN backbone was modified by several functionalities revealing the influences on thermal, energetic and chemical properties. Mononitramino PETN **4** shows to be remarkably less

sensitive while the thermal stability and performance are largely maintained compared to PETN. Introducing tetrazoles to the PETN backbone, caused the resulting tristetrazole PETN **5** and tetrazole PETN **7** to be less friction sensitive. The formal addition of HCN on the azide of sensitive monoazido PETN causes the resulting tetrazole **5** to be less friction sensitive and shifts the melting point to 26 °C higher. Compounds **4**, **5** and **7** are candidates to replace TNT. However, compound **4** shows a low melting point and **5** and **7** are impact sensitive. Due to the low water solubility, the good sensitivity parameters and the high-performance mononitramino PETN **4** is particularly outstanding. Although their synthesis appears to be too complex, this study shows that methyl-bridged nitramine and tetrazoles should be considered for the synthesis of new melt cast energetic material. The introduction of the amine-like **3** or ionic groups like **3a**, **3b**, **4a**, **4b**, **9a**, **9b**, **9c** and **9d** has been shown to decrease the thermal properties but sometimes improve energetic properties.

Experimental Section

Compound 3: Compound **2** (500 mg, 3.70 mmol) was added in portions to HNO₃ (100%, 4 mL) at 0 °C–5 °C. The resulting mixture was stirred at this temperature for 15 min., then was allowed to warm to r.t. After 15 min the reaction mixture was poured on ice-water and neutralized with NaHCO₃. The solution was extracted with EtOAc (3 × 100 mL), the combined organic phases were dried over Na₂SO₄ and the solvent was removed under reduced pressure, to provide amine **3** (560 mg, 2.08 mmol, 56%) as a yellowish paste. DTA (5 °C min⁻¹): 89 °C (melt.), 153 °C (dec.), Sensitivities: BAM drop hammer: 7.5 J, BAM friction tester: 360 N, IR (ATR): ν_{\max} [cm⁻¹] = 2935 (w), 1630 (s), 1471 (m), 1374 (m), 1333 (m), 1272 (vs), 1259 (s), 1092 (m), 980 (s), 929 (m), 851 (vs), 826 (s), 753 (s), 725 (s), 715 (s), 613 (s), 591 (s), 557 (m), 418 (s), 411 (s), EA (C₅H₁₀N₄O₉, 270.15 g mol⁻¹): calc.: C 22.23, N 20.74, H 3.73%; found: C 22.63, N 20.18, H 3.75%, ¹H NMR (400 MHz, Methanol-*d*₄): δ (ppm) = 4.67 (s, 6H), 2.91 (s, 2H), ¹³C NMR (101 MHz, Methanol-*d*₄): δ (ppm) = 70.8, 51.1, 43.0.

Compound 4: Amine **3** (5.28 g, 39.1 mmol, 1.0 equiv.) was dissolved in H₂O (100 mL). Then half of the ethyl chloroformate (3.72 mL, 39.1 mmol, 1.0 equiv.) was added dropwise to the solution at 0 °C. Afterwards, KOH (2.19 g, 39.1 mmol, 1.0 equiv.) was dissolved in H₂O (120 mL). The potassium hydroxide solution and the remaining ethyl chloroformate were then added dropwise in an alternating manner. The solution was stirred overnight at room temperature. The solvent was removed by a rotation evaporator and a white residue was obtained. This residue was then extracted with EtOH (50 mL) (formed KCl is not soluble). The EtOH then was removed under reduced pressure and compound **4_prec1** was obtained as a white solid (3.98 g, 19.2 mmol, 49%). ¹H NMR (400 MHz, DMSO-*d*₆): δ (ppm) = 6.74 (t, *J* = 6.1 Hz, 1H), 4.27 (t, *J* = 5.4 Hz, 3H), 3.98 (q, *J* = 7.1 Hz, 2H), 3.29 (d, *J* = 4.9 Hz, 6H), 2.99 (d, *J* = 6.2 Hz, 2H), 1.15 (t, *J* = 7.1 Hz, 3H); ¹³C NMR (101 MHz, DMSO-*d*₆): δ (ppm) = 157.2, 61.0, 59.9, 45.1, 40.9, 14.6. Then fuming HNO₃ (99%, 12 mL) was added slowly to TFAA (24 mL) at 5 °C. Compound **4_prec1** (0.93 mg, 4.50 mmol) was added in portions at 5–10 °C. The yellow solution was then stirred at room temperature overnight. The either orange or clear solution was then added onto ice (50 mL) and extracted with DCM (3 × 50 mL). The organic phase was then washed with sat. NaHCO₃ solution (3 × 100 mL) and with brine (1 × 100 mL). After drying over Na₂SO₄ the solvent was removed under reduced pressure. Yellowish-white solid **4_prec2** was obtained (1.36 g,

3.51 mmol, 78%). $^1\text{H NMR}$ (400 MHz, $\text{DMSO-}d_6$): δ (ppm) = 4.67 (s, 6H), 4.41 (s, 2H), 4.31 (q, $J = 7.1$ Hz, 2H), 1.28 (t, $J = 7.1$ Hz, 3H); $^{13}\text{C NMR}$ (101 MHz, $\text{DMSO-}d_6$): δ (ppm) = 150.7, 71.0, 65.2, 49.0, 42.2, 13.6. Then compound (**4_prec2**) (1.71 g, 3.74 mmol, 1.0 equiv.) was dissolved in Et_2O (50 mL). Afterwards, NH_3 -gas was passed into the solution for 20 min. Then the suspension was extracted with water (3×25 mL). The aqueous phase was acidified carefully with HCl (2 M). The solution was extracted with EtOAc (3×25 mL). The organic phase was dried over Na_2SO_4 , filtered and the solvent was removed. Compound **4** was obtained as a white solid (676 mg, 2.14 mmol, 78%). DTA (5°C min^{-1}): 64 (melt.), 170°C (dec.); Sensitivities ($< 500 \mu\text{m}$, crystalline material): BAM drop hammer: 10 J; BAM friction tester: > 360 N; IR (ATR): ν_{max} [cm^{-1}] = 3318 (w), 2903 (w), 1631 (vs), 1590 (s), 1393 (m), 1322 (s), 1265 (vs), 1023 (s), 994 (s), 839 (vs), 752 (s), 702 (s), 622 (s), 526 (s); EA ($\text{C}_5\text{H}_9\text{N}_5\text{O}_{11}$, $315.15 \text{ g mol}^{-1}$): calc.: C 19.06, N 22.22, H 2.88%; found: C 19.31, N 21.95, H 2.73%; $^1\text{H NMR}$ (400 MHz, $\text{DMSO-}d_6$): δ (ppm) = 12.32 (s, 1H), 4.61 (s, 6H), 3.78 (s, 2H); $^{13}\text{C NMR}$ (101 MHz, $\text{DMSO-}d_6$): δ (ppm) = 71.0, 44.1, 41.9; $^{15}\text{N NMR}$ (41 MHz, $\text{Acetone-}d_6$): δ (ppm) = -27.2, -45.0, -215.7.

Compound 5: Amine **3** (1.00 g, 7.39 mmol, 1.0 equiv.), NaN_3 (578 mg, 8.89 mmol, 1.2 equiv.) and triethyl orthoformate (1.84 mL, 11.07 mmol, 1.5 equiv.) were added together and then heated at 40°C . Dropwise AcOH (4 mL) was added and the solution was heated at 85°C for 3 h. Afterwards conc. HCl (0.75 mL, 9.00 mmol, 1.2 equiv.) was added slowly. The obtained suspension was filtered off, and conc. HCl (10 mL) was added to the filtrate. After heating at 60°C for 30 min. the solvent was removed under vacuum to obtain **5_prec1**. $^1\text{H NMR}$ (400 MHz, $\text{DMSO-}d_6$): δ (ppm) = 9.21 (s, 1H), 4.41 (s, 2H), 3.26 (s, 6H), $^{13}\text{C NMR}$ (101 MHz, $\text{DMSO-}d_6$): δ (ppm) = 145.6, 60.4, 46.2, 45.7. This crude material was added in portions to HNO_3 (99%, 8 mL) at 0°C – 5°C . The resulting mixture was stirred at 0°C for 15 min., was allowed to warm to r.t. and stirred for another 15 min. Then the reaction mixture was poured on ice-water and neutralized with NaHCO_3 . After extraction with EtOAc (3×50 mL), the combined organic phases were dried over Na_2SO_4 and the solvent was removed under reduced pressure. The resulting crude was then purified via column chromatography (*i*-Hex/EtOAc, 1:1) to afford colorless solid **5** (974 mg, 3.01 mmol, 41%). DTA (5°C min^{-1}): 106°C (melt.), 180°C (dec.), Sensitivities: BAM drop hammer: 2 J; BAM friction tester: 160 N, IR (ATR): ν_{max} [cm^{-1}] = 3154 (w), 3026 (vw), 2992 (vw), 2904 (w), 1626 (vs), 1467 (m), 1389 (w), 1275 (vs), 1171 (m), 1124 (w), 1096 (m), 1036 (m), 1007 (s), 985 (m), 962 (w), 856 (vs), 773 (m), 753 (s), 729 (m), 709 (s), 696 (m), 661 (m), 631 (m), 623 (m), 454 (m), EA ($\text{C}_6\text{H}_9\text{N}_7\text{O}_9$, $323.18 \text{ g mol}^{-1}$): calc.: C 22.30, N 30.34, H 2.81%; found: C 22.32, N 30.08, H 2.73%, $^1\text{H NMR}$ (400 MHz, $\text{DMSO-}d_6$): δ (ppm) = 9.53 (s, 1H), 4.82 (s, 2H), 4.66 (s, 6H); $^{13}\text{C NMR}$ (101 MHz, $\text{DMSO-}d_6$): δ = 145.5, 70.6, 46.9, 41.3; $^{15}\text{N NMR}$ (41 MHz, Acetone): δ (ppm) = 11.0 (d, $J = 3.1$ Hz), -16.6 (s), -50.0 (t, $J = 1.9$ Hz), -54.9 (d, $J = 12.2$ Hz), -156.7 (d, $J = 9.7$ Hz).

Compound 7: Compound **6** (1.00 g, 5.74 mmol) was added in portions to HNO_3 (99%, 8 mL) at 0°C – 5°C . The resulting mixture was stirred at 0°C for 15 min., was allowed to warm to ambient temperature and stirred for another 15 min. Then the reaction mixture was poured on ice-water and neutralized with NaHCO_3 . After extraction with EtOAc (3×50 mL), the combined organic phases were dried over Na_2SO_4 and the solvent was removed under reduced pressure leaving colorless crystalline **7** (1.10 g, 3.56 mmol, 62%). DTA (5°C min^{-1}): 92°C (melt.), 163°C (dec.), Sensitivities: BAM drop hammer: 2 J; BAM friction tester: 80 N, IR (ATR): ν_{max} [cm^{-1}] = 3123 (w), 3026 (w), 2922 (w), 1641 (vs), 1380 (m), 1296 (m), 1280 (vs), 1259 (s), 1093 (m), 1035 (s), 1021 (s), 977 (m), 866 (s), 836 (vs), 751 (s), 740 (s), 725 (s), 714 (s), 624 (s), 557 (m); EA ($\text{C}_5\text{H}_7\text{N}_7\text{O}_9$, $309.15 \text{ g mol}^{-1}$): calc.: C 19.43, N 31.72, H 2.28%; found: C 19.79, N 30.40, H 2.45%, $^1\text{H NMR}$ (400 MHz, $\text{Acetone-}d_6$): δ (ppm) = 9.68 (s,

1H), 5.47 (s, 6H); $^{13}\text{C NMR}$ (101 MHz, $\text{Acetone-}d_6$): δ (ppm) = 143.6, 69.9, 62.4; $^{15}\text{N NMR}$ (41 MHz, $\text{Acetone-}d_6$): δ (ppm) = 13.3, -18.4, -49.0, -50.7, -145.1.

CCDC

Deposition Number(s) 2236739 (for **2_CO2**), 2232124 (for **3a**), 2232126 (for **3b**), 2232127 (for **4a**), 2232121 (for **4b**), 2232120 (for **5**), 2232116 (for **5_acetyl**), 2232122 (for **7**), 2232125 (for **8**), 2232123 (for **9**), 2232117 (for **9_prec1**), 2232118 (for **9_prec2**), 2232128 (for **9a**), 2232119 (for **9b**) contain(s) the supplementary crystallographic data for this paper. These data are provided free of charge by the joint Cambridge Crystallographic Data Centre and Fachinformationszentrum Karlsruhe Access Structures service.

Acknowledgements

For financial support of this work by Ludwig-Maximilian University (LMU), the Office of Naval Research (ONR) under grant no. ONR N00014-19-1-2078 and the Strategic Environmental Research and Development Program (SERDP) under contract no. W912HQ19C0033 are gratefully acknowledged. We thank Prof. Dr. Konstantin Karaghiosoff for the measurement of the ^{15}N NMR spectra and Dr. Peter Mayer for his help with X-ray crystallography measurements. Open Access funding enabled and organized by Projekt DEAL.

Conflict of Interest

The authors declare no conflict of interest.

Data Availability Statement

The data that support the findings of this study are available in the supplementary material of this article.

Keywords: energetic materials · meltcast · nitramine · PETN · tetrazole

- [1] E. Berlow, R. H. Barth, J. E. Snow, *The Pentaerythritols*, Reinhold Publishing Corporation, New York, 1958.
- [2] a) T. M. Klapötke, *Chemistry of High-Energy Materials*, 6th Ed., Walter de Gruyter GmbH, Berlin/Boston, 2022; b) R. M. J. Köhler, A. Homburg, *Explosivstoffe*, Vol. 10, WILEY-VCH Verlag GmbH, Weinheim, 2008; c) J. P. Agrawal, *High Energy Materials*, WILEY-VCH Verlag GmbH & Co., Weinheim, 2010.
- [3] a) T. Blessinger, L. D'Amico, R. Subramaniam, C. Brinkerhoff in *EPA/635/R-18/211Fa*, U. S. Environmental Protection Agency, Washington, 2018; b) Technical Fact Sheet - 2,4,6-Trinitrotoluene (TNT) in *EPA 505-F-21-001*, U. S. Environmental Protection Agency, Washington, 2021.
- [4] P. A. Persson, *US 4220087 A*, 1971.
- [5] a) A. E. Terhemen, *Adv. J. Chem., Sect. A* 2020, 3, 122–130; b) S. V. Bondarchuk, *FirePhysChem* 2022, 2, 160–167; c) S. Song, F. Chen, Y. Wang, K. Wang, M. Yan, Q. Zhang, *J. Mater. Chem.* 2021, 9, 21723–21731.
- [6] a) F. W. Marrs, V. W. Manner, A. C. Burch, J. D. Yeager, G. W. Brown, L. M. Kay, R. T. Buckley, C. M. Anderson-Cook, M. J. Cawkwell, *Ind. Eng. Chem. Res.* 2021, 60, 5024–5033; b) P. J. Rae, P. M. Dickson, *J. Dynamic Behavior Mater.* 2021, 7, 414–424.

- [7] J. M. Winey, K. Zimmerman, Z. A. Dreger, Y. M. Gupta, *J. Phys. Chem. A* **2020**, *124*, 6521–6527.
- [8] a) Virginia, W. Manner, M. J. Cawkwell, E. M. Kober, T. W. Myers, G. W. Brown, H. Tian, C. J. Snyder, R. Perriot, D. N. Preston, *Chem. Sci.* **2018**, *9*, 3649–3663; b) T. W. Myers, C. J. Snyder, V. W. Manner, *Cryst. Growth Des.* **2017**, *17*, 3204–3209.
- [9] a) Y.-H. Joo, J. M. Shreeve, *Chem. Commun.* **2010**, *46*, 142–144; b) R. P. Singh, J. M. Shreeve, *Chem. Eur. J.* **2011**, *17*, 11876–11881.
- [10] a) N. Lease, V. W. Manner, D. E. Chavez, D. Robbins, L. Kay, *AIP Conf. Proc.* **2020**, 2272, 050013; b) N. Lease, L. M. Kay, G. W. Brown, D. E. Chavez, D. Robbins, E. F. C. Byrd, G. H. Imler, D. A. Parrish, V. W. Manner, *J. Org. Chem.* **2020**, *85*, 4619–4626.
- [11] T. Lenz, T. M. Klapötke, M. Mühlemann, J. Stierstorfer, *Propellants Explos. Pyrotech.* **2021**, *46*, 723–731.
- [12] a) D. E. Chavez, M. A. Hiskey, D. L. Naud, D. Parrish, *Angew. Chem. Int. Ed.* **2008**, *47*, 8307–8309; *Angew. Chem.* **2008**, *120*, 8431–8433; b) T. W. Myers, C. J. Snyder, D. E. Chavez, R. J. Scharff, J. M. Veauthier, *Chem. Eur. J.* **2016**, *22*, 10590–10596.
- [13] J. J. Sabatini, E. C. Johnson, *ACS Omega* **2021**, *6*, 11813–11821.
- [14] E. C. Johnson, J. J. Sabatini, D. E. Chavez, R. C. Sausa, E. F. C. Byrd, L. A. Wingard, P. E. Guzmàn, *Org. Process Res. Dev.* **2018**, *22*, 736–740.
- [15] S. Wawzonek, A. Matar, C. H. Issidorides, *Org. Synth.* **2003**, *38*, 68–68.
- [16] M. A. Hiskey, M. J. Hatch, J. C. Oxley, *Propellants Explos. Pyrotech.* **1991**, *16*, 40–42.
- [17] T. Altenburg, T. M. Klapötke, A. Penger, *Cent. Eur. J. Energ. Mater.* **2009**, *6*, 255–275.
- [18] “Formation of the potassium salt in Ethanol yielded crystals of potassium nitrite.”
- [19] P. N. Gaponik, V. P. Karavai, Y. V. Grigor’ev, *Chem. Heterocycl. Compd.* **1985**, *21*, 1255–1258.
- [20] a) M. Benz, T. M. Klapötke, T. Lenz, J. Stierstorfer, *Chem. Eur. J.* **2022**, *28*, e202200772; b) M. S. Gruhne, T. Lenz, M. Rösch, M. Lommel, M. H. H. Wurzenberger, T. M. Klapötke, J. Stierstorfer, *Dalton Trans.* **2021**, *50*, 10811–10825.

Manuscript received: December 22, 2022

Accepted manuscript online: January 24, 2023

Version of record online: March 10, 2023